

Article

Evaluation of Mechanical and Shrinkage Behavior of Lowered Temperatures Cementitious Mortars Mixed with Nitrite–Nitrate Based Accelerator

Yusuke Tomita ¹, Akira Yoneyama ¹, Heesup Choi ^{1,*} , Masumi Inoue ¹, Jihoon Kim ², Hyeonggil Choi ³ and Yuhji Sudoh ⁴

¹ Department of Civil and Environmental Engineering, Kitami Institute of Technology, Hokkaido 090-8507, Japan; m2052200130@std.kitami-it.ac.jp (Y.T.); m1952200234@std.kitami-it.ac.jp (A.Y.); m-inoue@mail.kitami-it.ac.jp (M.I.)

² Faculty of Environmental Technology, Muroran Institute of Technology, Hokkaido 090-8585, Japan; bmjhun@mmm.muroran-it.ac.jp

³ School of Architecture, Civil, Environment, and Energy Engineering, Kyungpook National University, Daegu 41566, Korea; hgchoi@knu.ac.kr

⁴ Basic Chemicals Department Chemicals Division, Nissan Chemical Corporation, Tokyo 103-6119, Japan; sudouyuuji@nissanchem.co.jp

* Correspondence: hs-choi@mail.kitami-it.ac.jp

Received: 23 July 2020; Accepted: 18 August 2020; Published: 20 August 2020



Abstract: Recently, calcium nitrite ($\text{Ca}(\text{NO}_2)_2$) and calcium nitrate ($\text{Ca}(\text{NO}_3)_2$) have been increasingly used as the main components of salt- and alkali-free anti-freezing agents, for promoting concrete hydration in cold-weather concreting. With an increase in the amount of nitrite-based accelerator, the hydration of C_3A , C_3S , and $\beta\text{C}_2\text{S}$ in the cement is accelerated, thereby improving its early strength and effectively preventing the initial frost damage. Meanwhile, with an increase in the amount of nitrite-based accelerator, the expansion and shrinkage of the concrete—and, therefore, the crack occurrence—are expected to increase. In this study, various experiments were conducted on shrinkage, crack initiation, and the development of mortar containing a considerable amount of a nitrite-based accelerator. The result confirmed that, as the amount of nitrite-based accelerator was increased, the shrinkage was increased, and cracking in early age was more likely to occur, compared to the cases without the addition of this accelerator.

Keywords: frost-resistant accelerator; calcium nitrite; calcium nitrate; cracking; strength; pore volume; shrinkage; crack potential; degree of restraint

1. Introduction

During cold-weather concreting, to prevent the initial frost damage, it is necessary to control the temperature until the concrete strength reaches 5 N/mm^2 of the heat curing, using a temporary enclosure and heater [1–6]. On the other hand, under a very low temperature or worse conditions—such as a steep incline, narrow space, or windstorm—anti-freezing agents are used to prevent the initial frost damage and secure the initial strength by sheet curing. Generally, the allowable range of anti-freezing agents is from -4 to $-8 \text{ }^\circ\text{C}$ [7–10]. However, when the daily average temperature is below $-10 \text{ }^\circ\text{C}$, it is necessary to increase the amount of anti-freezing agent.

At present, calcium nitrite and calcium nitrate are used as the main components of a salt- and alkali-free-type nitrite-based accelerator (CN) [9,10]. It has been proposed that increasing the amount of this nitrite-based accelerator contributes to good initial strength development in low-temperature environments, due to the hydration promotion of C_3A in the cement—and that is due to the increased

solubility of C_3S and βC_2S [11–13]. According to the Japanese Architectural Standard Specification for Reinforced Concrete Work (JASS5), shrinkage cracks need to be reduced to ensure the durability of concrete. Therefore, the drying shrinkage rate of concrete has been stipulated to be under 8×10^{-4} [14].

CN accelerates the hydration reaction of the C_3A contained in cement and increases the amount of ettringite and monosulfate [15–17]. This is because hydrates, such as nitrite–nitrate hydrate ($3CaO \cdot Al_2O_3 \cdot Ca(NO_2/NO_3)_2 \cdot xH_2O$), are formed through reactions between the C_3A (Al_2O_3), NO_2^- , and NO_3^- in CN [15–17]. Therefore, the chemical shrinkage potential of the cement matrix increases, which leads to a higher concern regarding shrinkage cracking. However, few studies have focused on shrinkage cracking.

In this study, the authors' aims are to clarify the shrinkage behavior of concrete, and the initiation and development of cracks, when a considerable amount of CN is present in the mixture. Therefore, various experiments have been conducted to quantitatively evaluate the physical and shrinkage cracking properties of mortar containing a considerable amount of CN. Figure 1 shows the flowchart for this study.

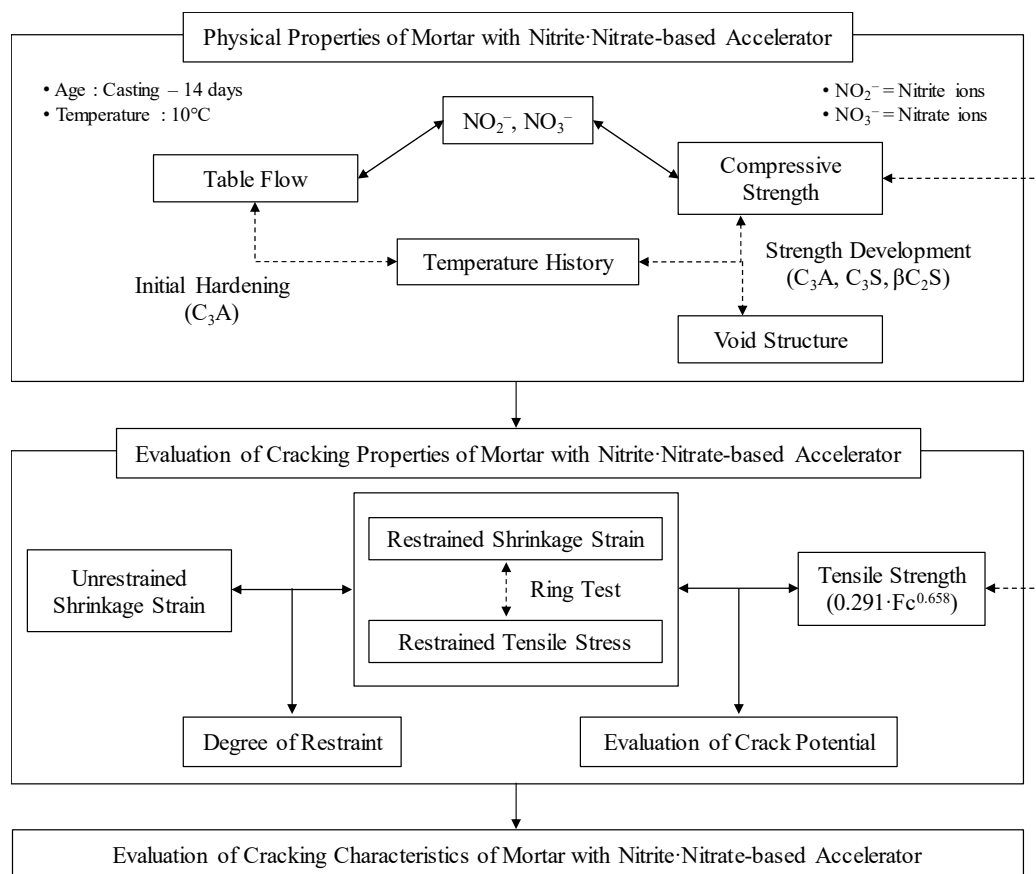


Figure 1. Study flow chart.

2. Experimental Overview

2.1. Materials and Procedures

Table 1 presents the materials used in the experiments conducted in this study, and Table 2 presents their CN components. CN is a 45% mixed aqueous solution of calcium nitrite and calcium nitrate. Table 3 presents the mortar composition used in the experiments, where the water–cement ratio is 50% and the sand–cement ratio (S/C) is 2.5 [10,11]. The standard amount of accelerator added is 4%–7% of the cement mass, depending on the ambient temperature [10]. Assuming a case where a considerable amount of CN was added in extremely low temperatures, the amount of CN added was

set to the four levels of 0, 7, 9, and 11%, as compared to the cement weight. The concrete temperature during the unloading has been specified as 10~20 °C by the Architectural Institute of Japan in the Recommendation for Practice of Cold Weather Concreting (Practical Guideline for Investigation (2010)). Therefore, in the experiment, to elucidate the behavioral assessment of the concrete expansion and shrinkage when a CN is added, both mixing and sealed curing were performed at 10 ± 1 °C and $85\% \pm 5\%$ (Relative Humidity; RH), from Day 1 to Day 14, after placing.

Table 1. Properties of the materials used (Data from [18]).

Materials (Code)	Properties
Cement (C)	Normal Portland cement, density: 3.16 g/cm ³ (Taiheiyo Cement, Tokyo, Japan)
Fine aggregate (S)	No. 5 silica sand, absolute dry density: 2.61 g/cm ³ , Water absorption: 0.26%, fineness modulus: 2.16 (Tochu, Tokyo, Japan)
Anti-freezing agent (CN)	Nitrite nitrate-based accelerator = calcium nitrite (Ca(NO ₂) ₂); calcium nitrate (Ca(NO ₃) ₂) (Nissan Chemical, Tokyo, Japan)

Note: CN: Anti-freezing agent = nitrite + nitrate-based accelerator (Ca(NO₂)₂ + Ca(NO₃)₂).

Table 2. Properties of the anti-freezing agent (Data from [18]).

Code	Component	Component Ratio	pH	Specific Gravity
CN	Ca(NO ₂) ₂	23.02%	9.3	1.43 g/cm ³
	Ca(NO ₃) ₂	22.81%		

Table 3. Proportions of the mortar mix (Data from [18]).

Type	W/C (%)	S/C	Unit Content (kg/m ³)			Anti-Freezing Agent (C × %)
			W	C	S	CN
CN0	50	2.5	281	562	1407	0
CN7						7
CN9						9
CN11						11

Note: W/C: Water–cement ratio; S/C: Sand–cement ratio; CN0: Mixing amount of anti-freezing agent = 0%; CN7: Mixing amount of anti-freezing agent = 7%; CN9: Mixing amount of anti-freezing agent = 9%; CN11: Mixing amount of anti-freezing agent = 11%.

2.2. Experimental Method

As the amount of nitrite-based accelerator was increased, various physical and shrinkage behavior assessments were conducted at various ages, using the experimental method outlined below. Table 4 shows the conditions and assessment method applied in this experiment.

Table 4. Experimental conditions and evaluation method (Data from [18]).

Temperature Condition	Experimental Period	Subject and Method of Evaluation	
		Physical Properties	Shrinkage Properties
10 °C	Casting—14 days	Flow test	Un/Restrained shrinkage
		Compressive strength	Tensile strength
		Temperature history	Crack potential
		MIP	Degree of restraint

Note: Physical and shrinkage properties: All cases; flow test: Immediately after placement; temperature history: Casting—14 days.

The mortar's fresh property was according to the "Flow test" in JIS R 5201 (Physical Testing Methods for Cement; Tokyo, Japan), and a flow test was performed immediately after mixing [19].

To assess the compressive strength, sealed curing was performed at 10 ± 1 °C and $85\% \pm 5\%$ RH, from Day 1 to Day 14, after placing the mortar into a $\phi 5 \times 10$ cm² mold. Next, the compressive strength was measured on Days 1, 3, 7, and 14.

For the internal temperature, a thermocouple (Tokyo, Japan) was installed at the center of a mold of 10×20 cm², and the time-dependent change in the mortar temperature immediately after mixing, until Day 14, was measured.

For the MIP (Mercury Intrusion Porosimetry) test, as shown in Figure 2, in order to obtain a sample that is representative of the measurement of porosity, samples were collected at each age and cut into 5 mm cubes. Then, in order to stop the hydration of the sample, the sample was immersed in acetone for 4 h or more, and dried by the D-dry method for 1 week, and then the pore distribution of each sample was measured at a minimum diameter of 6 nm, with a maximum pressure of 220 MPa.

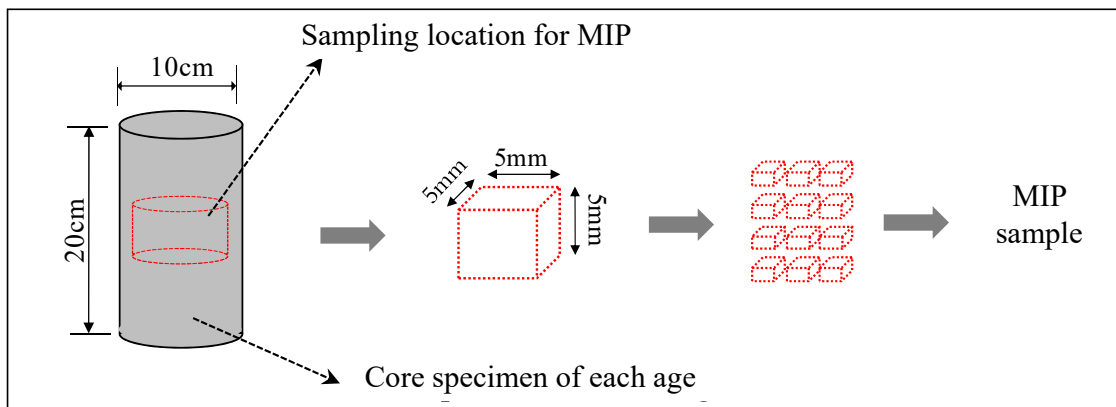


Figure 2. Sampling of specimen for evaluation of pore structure.

As shown in Figure 3, the unrestrained drying shrinkage strain was measured by embedding a reinforcing bar with a strain gauge that was attached to the center of a $10 \times 10 \times 40$ cm³ mold. To make the drying conditions identical to those of the ring specimen, and after demolding the specimen at the age of 1 day, the exposed surface area ratio was adjusted to be the same as that of the ring specimen (~44%) by covering the circumferential direction with aluminum tape.

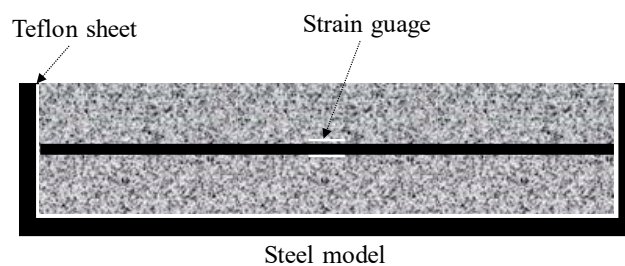


Figure 3. Overview of unrestrained drying shrinkage.

The restraint shrinkage strain is a strain generated by the restraint of the inner steel ring. The height of the ring test piece was changed from 152 to 75 mm, proposed by AASHTO (American Association of State Highway Transportation Officials; 1998), to induce uniform dry shrinkage at the cross-section of the concrete ring (Figure 4) [20,21]. In this experiment, a Teflon sheet was installed between the outer ring and the mortar to minimize the restraint from the outer ring and prevent water evaporation on the upper part of the test body. At the age of 1 day, the lower wood plate and upper Teflon sheet of the ring specimen were removed, and thus, only the upper and lower surfaces were dried. For determining the restrained shrinkage strain, strain gauges were attached at three locations ($h/2 = 37.5$ mm) in the center of the inner ring, and the change in the strain with time was measured immediately after that. Figure 5 shows the apparatus of the unrestrained drying shrinkage test, with the specimen's exposed surface

area ratio adjusted to be the same as that of the ring specimen. Figure 6 shows the apparatus of the restrained shrinkage test (ring test).

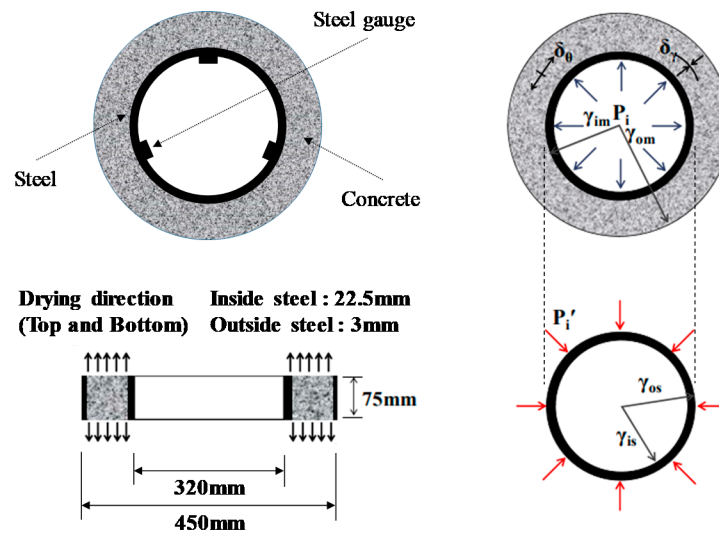


Figure 4. Overview of ring test (restrained shrinkage).

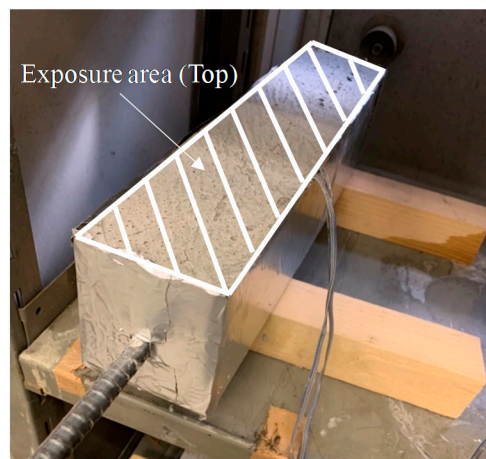


Figure 5. Unrestrained drying shrinkage.



Figure 6. Restrained shrinkage (ring test).

3. Physical Properties of Mortar with CN

3.1. Fresh Properties

Figure 7 shows the results of the table flow test in each case. The flow value of CN0 was set to 186 mm, based on those of CN7, CN9, and CN100, which were decreased by 6.5, 9.2, and 25.9%, respectively. As the amount of CN was increased, the flow value tended to decrease. Figure 8 shows the history of the internal temperature of the mortar (~2 h). The temperature peaks were 15.2 °C for CN0, 17.1 for CN7, 18.6 for CN9, and 22.0 for CN11. As the amount of CN was increased, the temperature tended to increase. When CN was added, the NO_2^- and NO_3^- reacted rapidly with the C_3A in the cement to produce nitrite/nitrate hydrate [13,15,17,18,22]. These results indicate that when a considerable amount of CN is added, hydration is promoted, the mortar temperature increases, and the flow value decreases.

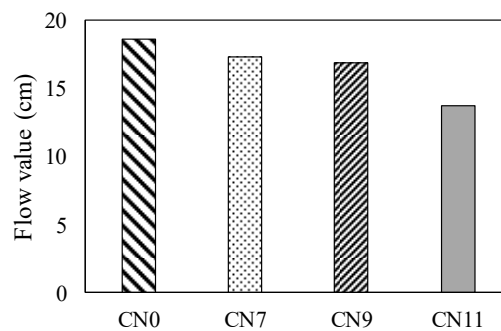


Figure 7. Flow value.

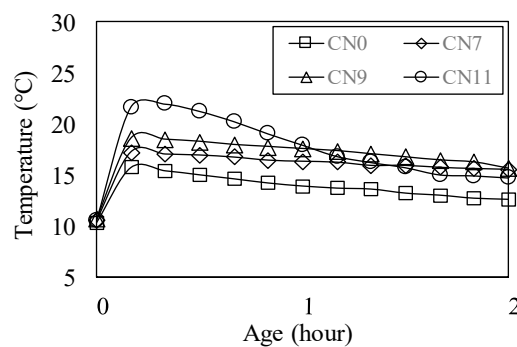


Figure 8. Temperature history (up to 2 h).

3.2. Compressive Strength Properties

Figure 9 shows the compressive strength from 1 to 14 days for each case. The compressive strength on Day 1 was 4.38 N/mm^2 for CN0, 5.15 for CN7, 6.51 for CN9, and 7.03 for CN11, and tended to increase with the amount of CN. Figure 10 shows the history of the mortar's internal temperature (~24 h). In particular, the temperature peaks at 0–4 h and 6–18 h increased [16], and the time required to reach the peak decreased. With an increase in the amount of CN, the temperature tended to increase; moreover, the amounts of NO_2^- and NO_3^- increased and reacted rapidly with the C_3A in the cement, which promoted hydration, increased the mortar temperature, and increased the amount of nitrite/nitrate hydrate. Therefore, the strength on Day 1 was considered to have increased. However, the compressive strength, by Day 3, tended to decrease as the amount of CN was increased. Furthermore, this tendency became remarkable after 7 days, and the strength in the case of CN addition was below that of CN0. With an increase in the amount of CN, the amounts of ettringite and nitrite/nitric acid hydrate produced also increased. Therefore, on Day 1, the structure became dense and the strength increased. After 3 days, when CN was added, a considerable amount of H_2O was consumed, with an increase in the amount of nitrite/nitrate hydrate [15,17,18,22]. This relatively

reduced the amounts of C-S-H and Ca(OH)₂ produced by the reaction in ordinary cement, and made the structure without CN denser than that with CN. Therefore, the strength was considered to increase.

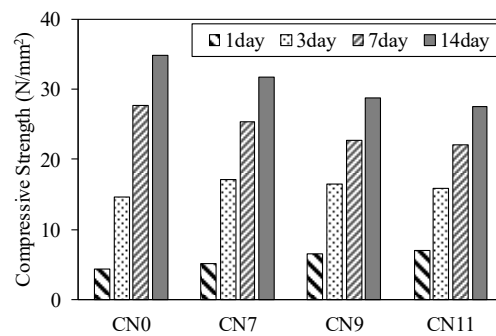


Figure 9. Compressive strength.

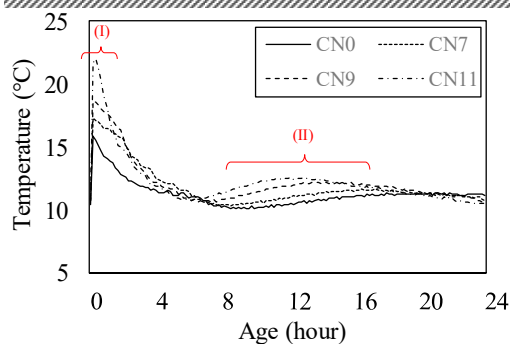


Figure 10. Temperature history (up to 24 h).

3.3. Void Structure Properties

Figure 11 shows the void distribution on Day 1, where CN1 had a void distribution in the range of 0.5 to 5 μm, CN7 from 0.1 to 3 μm, CN9 from 0.05 to 0.5 μm, and CN11 from 0.03 to 0.1 μm. According to these results, the void diameter and volume tended to decrease as the amount of CN added was increased. In particular, in the cases of a considerable amount of CN being added (CN9 and CN11), many voids were formed within the range of 0.05 μm or less, which was considered to substantially affect dry shrinkage [16]. Figure 12 shows the void distribution by Day 14. In all cases, the void volume tended to be smaller than that on Day 1. These results indicate that CN addition increased the amount of nitrite/nitrate hydrate produced immediately after mixing, and promoted hydration; moreover, the voids were filled, resulting in a good strength on Day 1. On the other hand, after 14 days, there was no clear relationship between the void structure and the fact that the case of CN addition had a lower compressive strength than that with no addition of CN.

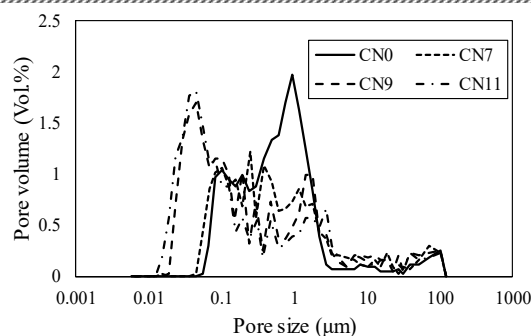


Figure 11. Void distribution (1 day).

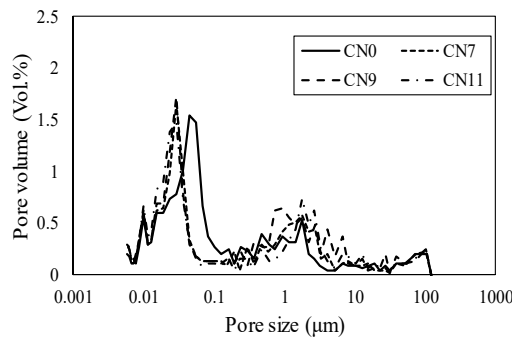


Figure 12. Void distribution (14 days).

4. Shrinkage Properties of Mortar with CN

4.1. Restrained Drying Shrinkage

Figure 13 shows the restrained shrinkage strain results obtained for the ring test. Table 5 shows the occurrence of cracks in each test piece and the number of days until the crack occurred. First, the shrinkage started after casting, after ~10 h for CN11, 11 h for CN9, 12 h for CN11, and 36 h for CN0. In particular, in the case of CN addition, shrinkage gradually occurred ~6 h after casting, after which cracks occurred in the process of increasing shrinkage. The cracking dates were 2.8 days for CN11, 3.6 days for CN9, and 4.4 days for CN7. The cracks tended to occur faster as the amount of CN was increased. The restrained shrinkage strains at the time of cracking were 25 µ for CN11, 27 µ for CN9, and 30 µ for CN7. On the other hand, in the case of CN0, no cracks occurred during the measurement period of this experiment.

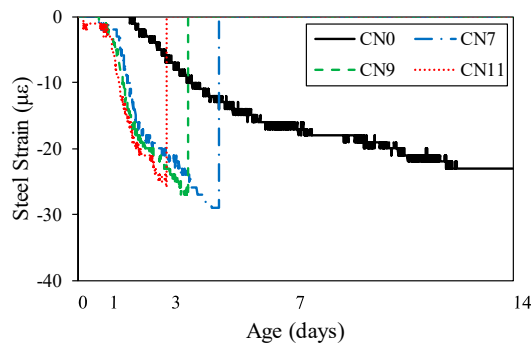
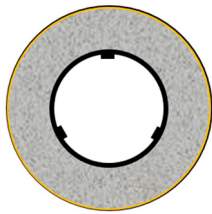
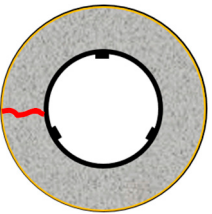
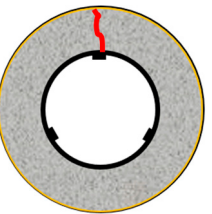
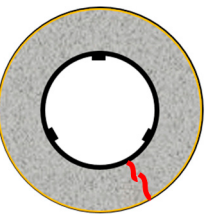


Figure 13. Restraint shrinkage.

Table 5. Crack configuration and cracking days.

Cracking				
Case	CN0	CN7	CN9	CN11
Days of Cracking	-	4.4 days	3.6 days	2.8 days

4.2. Restrained Tensile Stress and Crack Potential

The restrained tensile stress can be calculated by Equation (1) using the radii of the concrete and steel ring, restrained shrinkage strain, and elastic modulus of the steel ring, assuming that the concrete poured into the ring specimen had a uniform shrinkage in the shear plane with a linear behavior [21,23–25].

$$\sigma_{\theta_{imax}} = \frac{(\gamma_{os2} - \gamma_{is2}) \cdot (\gamma_{im2} + \gamma_{om2})}{2\gamma_{os2} \cdot (\gamma_{om2} - \gamma_{im2})} \cdot E_{st} \cdot \epsilon_{st} \tag{1}$$

Here, $\sigma_{\theta_{imax}}$ indicates the restrained tensile stress, γ_{is} and γ_{os} indicate the internal and external radii of the steel ring, γ_{ic} and γ_{oc} indicate the internal and external radii of the concrete, E_{st} indicates the elastic modulus, and ϵ_{st} indicates the restrained shrinkage strain.

Figure 14 shows the restrained tensile stress calculated by Equation (1), which tended to increase with the restraint shrinkage strain. The maximum restrained tensile stress was 1.8 N/mm² for CN11, 1.9 N/mm² for CN9, and 2.1 N/mm² for CN7, and cracking occurred after reaching the maximum tensile stress. The restrained tensile stress increased with the amount of CN added because of the increase in the stress generated in the inner steel ring. This was confirmed to accelerate the crack occurrence in the mortar. It is considered that the stress relaxation was reduced by the tensile creep. On the other hand, the cracking potential is calculated from the ratio of restrained tensile stress to tensile strength. Figure 15 shows the change in tensile strength over time, and Figure 16 shows the crack potential in each case. The tensile strength was calculated by Equation (2) using the result from the compressive strength [26]:

$$\sigma_B = 0.291 \cdot Fc^{0.658} \tag{2}$$

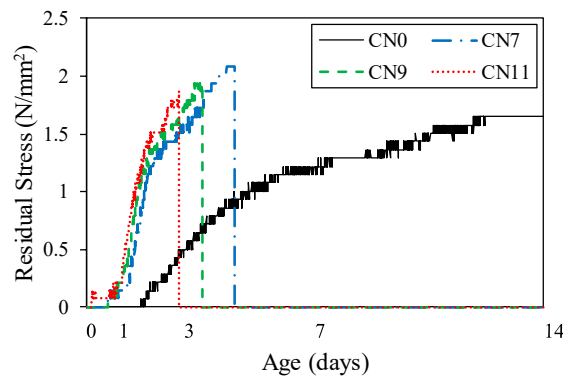


Figure 14. Restraint tensile stress.

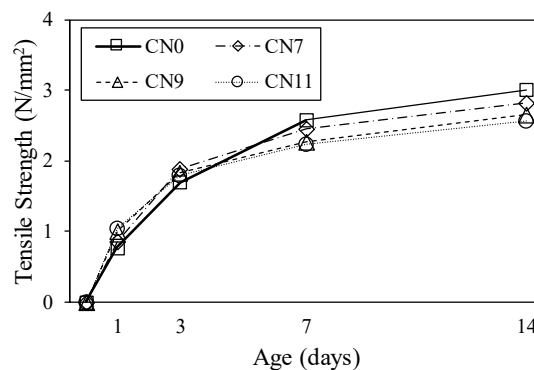


Figure 15. Tensile strength.

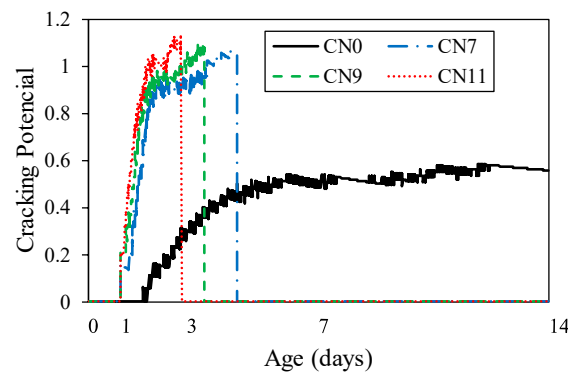


Figure 16. Cracking potential.

Here, σ_B refers to the tensile strength and F_c refers to the compressive strength.

In the case of CN addition, the cracking potential increased between the ages of 1 and 2 days. The possibility of crack occurrence became very high at an early age, compared to the case of no CN addition. According to this result, under the restraint conditions in this test, with an increase in the amount of CN added, both the shrinkage and crack occurrence possibility increased.

4.3. Degree of Restraint

Figure 17 shows the changes in the drying shrinkage strain over time. On Day 1, after the start of drying shrinkage, the drying shrinkage strain was 1.5 μ for CN0, 10.5 μ for CN7, 29 μ for CN9, and 36 μ for CN11, indicating that the drying shrinkage tended to increase with the amount of CN added. On Day 14, after the start of drying shrinkage, the drying shrinkage strain was 170 μ for CN0, 315 μ for CN7, 372 μ for CN9, and 430 μ for CN11, indicating that the drying shrinkage on Day 1 tended to increase with the amount of CN added, and became more pronounced. These results confirm that drying shrinkage increases with the amount of CN added, and agree with the restrained shrinkage results; moreover, when a considerable amount of CN was added, restrained shrinkage was considered to increase with drying shrinkage.

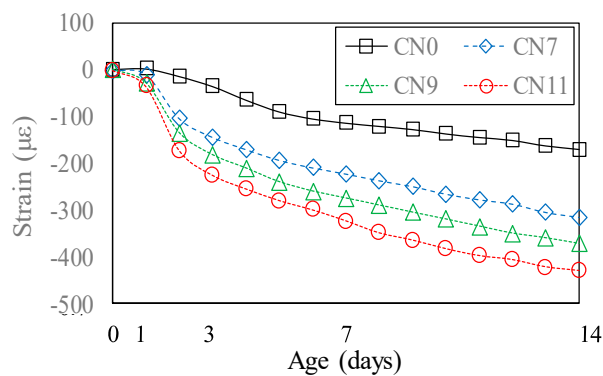


Figure 17. Unrestrained drying shrinkage.

Figure 18 shows the degree of restraint in the specimen by the restraining body which, in this test, was calculated using Equation (3), in order to evaluate the cracking [23–25].

$$\varphi = 1 - \frac{\varepsilon_{st}(t)}{\varepsilon_{sh}(t)} \tag{3}$$

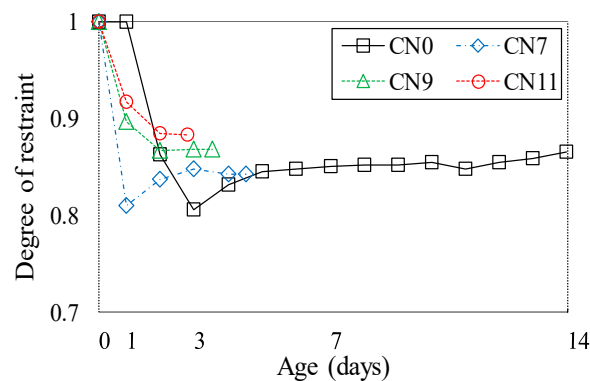


Figure 18. Degree of restraint.

Here, φ represents the degree of restraint, ε_{st} represents the amount of restrained shrinkage, and ε_{sh} represents the amount of drying shrinkage. ε_{st} is calculated by taking the concrete age of 0 days as the start of the restrained shrinkage.

The degree of restraint tended to increase slightly with the amount of CN added, and was ~ 0.84 for CN7, ~ 0.87 for CN9, and ~ 0.88 for CN11. This confirmed that the time the cracking occurred, caused by the degree of restraint, became earlier as the amount of CN added was increased. Meanwhile, in the specimen with no CN added, after decreasing to 0.80, the degree of restraint tended to gradually increase, reaching ~ 0.86 on Day 14. The results showed that when a considerable amount of CN was added, the cracking potential reached a maximum, and cracking occurred when the degree of restraint was between ~ 0.84 and 0.88. Therefore, it is considered necessary to examine the crack occurrence under the restraint conditions when using CN.

5. Conclusions

In this study, each experiment was conducted in order to clarify the shrinkage behavior and cracking of mortar when the amount of nitrite-based accelerator, used as an anti-freezing agent, was changed. The results are summarized as follows:

- (1) When the amount of CN was increased, hydration accelerated, the mortar temperature increased immediately after casting, and the fluidity decreased.
- (2) On Day 1, the addition of a considerable amount of CN promoted hydration and formed a large amount of nitrite/nitrite hydrate, resulting in dense voids and increased strength.
- (3) As the amount of CN was increased, shrinkage increased and its start time became earlier.
- (4) Under the restraint conditions in this study—from the results of the cracking potential and degree of restraint—as the amount of CN was increased, the shrinkage and crack occurrence possibility increased.

Author Contributions: Conceptualization, H.C. (Heesup Choi), J.K., and Y.S.; Data curation, J.K., A.Y.; Investigation, M.I., H.C. (Hyeonggil Choi), and Y.S.; Project administration, Y.T.; Supervision, H.C. (Heesup Choi); Supervision, H.C. (Heesup Choi); Writing—original draft, Y.T.; Writing—review & editing, H.C. (Heesup Choi). All authors have read and agreed to the published version of the manuscript.

Funding: This research received no external funding.

Acknowledgments: This research was supported by Nissan Chemical Co. of JAPAN.

Conflicts of Interest: The authors declare no conflict of interest.

References

1. Akama, T.; Inoue, M.; Sudoh, U.; Mikami, S. Fresh properties and early strength development of concrete using calcium nitrite and water-reducing agents. *Proc. Jpn. Concr. Inst.* **2012**, *34*, 155–159.
2. Taniguchi, M.; Nakamura, T.; Koike, S.; Nishi, H. Study on effect and mechanism of accelerator for freeze protection. *Hokkaido Res. Organ. North. Reg. Build. Res. Inst. (Res. Rep.)* **2015**, *358*, 1–11.
3. Hama, Y.; Kamada, E. The properties of concrete containing a frost-resistant accelerator. *Concr. J.* **1999**, *37*, 3–8. [[CrossRef](#)]
4. Hama, Y.; Kamada, E. Strength development under freezing conditions and freezing behavior of water in concrete with accelerators for freeze protection. *Concr. Res. Technol.* **1997**, *8*, 73–80. [[CrossRef](#)]
5. Nmai, C.K. Cold weather concreting admixtures. *Cem. Concr. Compos.* **1998**, *20*, 121–128. [[CrossRef](#)]
6. Polat, R.; Karagol, F.; Demirboga, R.; Kaygusuz, M.A.; Yadollahi, M.M. The influence of calcium nitrate as antifreeze admixture on the compressive strength of concrete exposed to low temperatures. *Cold Reg. Sci. Technol.* **2013**, *89*, 30–35.
7. Concrete Council of JSCE. *Standard Specifications for Concrete Structures-2017*; Japan Society of Civil Engineers: Tokyo, Japan, 2017. (In Japanese)
8. Practical Guideline for Investigation. *Recommendation for Practice of Cold Weather Concreting*; Architectural Institute of Japan: Tokyo, Japan, 2010. (In Japanese)
9. Kojima, T. *Concrete Admixture Handbook*; The Society of Materials Science: Tokyo, Japan, 2004; pp. 172–175. (In Japanese)
10. Construction Promotion Council. *Operation Manual of Anti-Freezing Agent*; Ministry of Land, Infrastructure, Transport and Tourism: Tokyo, Japan, 2005.
11. Iwasawa, M.; Inoue, M.; Choi, H.S.; Sudoh, Y. Study on fresh properties and strength development of mortar using nitrite-based accelerator and various water reducing agents. *Proc. Jpn. Concr. Inst.* **2018**, *40*, 243–248.
12. Choi, H. Control of curing temperature of cold-weather concrete through effective utilization of energy-saving heat-curing systems. In Proceedings of the 2017 World Congress on Advances in Structural Engineering and Mechanics, Seoul, Korea, 28 August–1 September 2017; pp. 1–8.
13. Ramachanran, V.S. *Concrete Admixture Handbook*; Noyes Publications: Park Ridge, NJ, USA, 1995; pp. 741–799.
14. Japanese Architectural Standard. *Specification for Reinforced Concrete Work JASS5*; Architectural Institute of Japan: Tokyo, Japan, 2018. (In Japanese)
15. Yukio, H.; Eiji, K. Effects on protection fresh concrete against frost damage by non-chloride and non-alkali type antifreezing admixtures. *Concr. Res. Technol.* **1996**, *7*, 113–122.
16. Paulo, J.M. *CONCRETE, Microstructure, Properties, and Materials*, 2nd ed.; Mc Graw Hill: New York, NY, USA, 1995; pp. 181–227.
17. Balonis, M.; Medala, M.; Glasser, F.P. Influence of calcium nitrate and nitrite on the constitution of AFm and Aft cement hydrates. *Adv. Cem. Res.* **2011**, *23*, 129–143. [[CrossRef](#)]
18. Heesup, C.; Masumi, I.; Hyeonggil, C.; Jihoon, K.; Yuhji, S.; Sukmin, K.; Bokyeong, L.; Akira, Y. Physicochemical study on the strength development characteristics of cold weather concrete using nitrite-nitrate-based accelerator. *J. Mater.* **2019**, *12*, 2706.
19. Japanese Industrial Standards. *Physical Testing Methods for Cement, JIS R 5201*; Japanese Standards Association: Tokyo, Japan, 2015; pp. 20–21.
20. Choi, H.G.; Lim, K.; Kitagaki, R.; Noguchi, T.; Kim, G.Y. Restrained shrinkage behavior of expansive mortar at early ages. *Constr. Build. Mater.* **2015**, *84*, 468–476. [[CrossRef](#)]
21. Hyeonggil, C.; Juncheol, L.; Bokyeong, L.; Jeongsoo, N. Shrinkage properties of concretes using blast furnace slag and frost-resistant accelerator. *Constr. Build. Mater.* **2019**, *220*, 1–9.
22. Jihoon, K.; Daiki, H.; Heesup, C.; Yukio, H. Investigation of the relationship between compressive strength and hydrate formation behavior of low-temperature cured cement upon addition of a nitrite-based accelerator. *J. Mater.* **2019**, *12*, 3936.
23. Hossain, A.B.; Weiss, W.J. Assessing residual stress development and stress relaxation in restrained concrete ring specimens. *Cem. Concr. Compos.* **2004**, *26*, 531–540. [[CrossRef](#)]

24. Weiss, W.J.; Fergeson, S. Restrained Shrinkage Testing: The Impact of Specimen Geometry on Quality Control Testing for Material Performance Assessment. In *Concreep 6, Creep, Shrinkage, and Durability Mechanic of Concrete and Other Quasi-Brittle Materials*; Ulm, F.J., Bazant, Z.P., Wittman, F.H., Eds.; Elsevier: Cambridge, UK, 2001; pp. 645–651.
25. Ugural, A.C.; Fenster, S.K. *Advanced Strength and Applied Elasticity*, 3rd ed.; Prentice Hall PTR, Inc.: New Jersey, NJ, USA, 1995; pp. 327–334.
26. Noguchi, T.; Tomozawa, F. Relationship between compressive strength and various mechanical properties of high strength concrete. *J. Struct. Constr. Eng.* **1995**, *60*, 11–16. [[CrossRef](#)]



© 2020 by the authors. Licensee MDPI, Basel, Switzerland. This article is an open access article distributed under the terms and conditions of the Creative Commons Attribution (CC BY) license (<http://creativecommons.org/licenses/by/4.0/>).